13th FIG Symposium on Deformation Measurement and Analysis
4th IAG Symposium on Geodesy for Geotechnical and Structural Engineering

LNEC, LISBON 2008 May 12-15

STRUCTURAL DEFORMATION OF THE HIGH-SPEED LINE (HSL) INFRASTRUCTURE IN THE NETHERLANDS; OBSERVATIONS USING SATELLITE RADAR INTERFEROMETRY

Mahmut ARIKAN and Ramon F. HANSSEN

Delft Institute of Earth Observation and Space Systems, Delft University of Technology, The Netherlands

Abstract: The Southern High-Speed Line (HSL), in Dutch known as *'HSL-Zuid,'* is a dedicated 125 km high-speed rail line, forming part of a new route between Antwerp, Belgium and Amsterdam. Construction began in 2000, and major engineering projects include the 7.2 km tunnel Leiderdorp-Hazerswoude under the *'Green Heart,'* an agricultural area between the country's four largest cities, Amsterdam, Rotterdam, The Hague and Utrecht. North of this tunnel, a section of the line near the city of Rijpwetering, containing the sharpest curve on the entire route, experienced significant structural deformation during the construction stage due to ground instability, and 800 m of the line had to be rebuilt. Local in-situ surveys show that up to 19 mm of horizontal deformation occurred after the reconstruction stage in 2006. Here we investigate whether local deformation of this kind can be observed by satellite radar interferometry, using a fine-tuned processing approach dedicated for this application. We report on the procedure followed, on the constraints in the parameter estimation and the obtained level of precision and reliability. The combination of a forward model to simulate radar observations from in situ measured displacements and an inverse model using the satellite data to estimate the displacements will be presented.

1. INTRODUCTION

The Southern High-Speed Line (HSL) is a dedicated 125 km high speed rail line connecting the Netherlands, especially an urban agglomerate of cities known as the *Randstad*, to numerous European economical centres, see Figure 1. People are increasingly willing to travel more but spend less time while travelling for business or for pleasure. Annually, about 14 million people are expected to travel by the HSL railway. In this aspect, the project is expected to accommodate most of the international heavy traffic to the Netherlands. The transportation along the HSL line is planned at a speed of 250 kilometres per hour on the domestic routes and at a top speed of 300 kilometres per hour on the route of Amsterdam to Paris. Between the both centres, the travel time is expected to decrease to three hours. Additionally, the project is competitive in medium-range travel, such as with cars and aeroplanes, with its reduction of road and air traffic in favour of environmental friendly transportation (HSL-Zuid, 2008).

Figure 1 - The route of the HSL in the Netherlands (HSL-Zuid)

Since the start of construction in 2000, the project undergoes heavy inspections to meet the Europeans safety and quality standards. In this way, the Dutch government aims to secure that the project is properly constructed with no unnecessary costs in the future and lasts at least 100 years.

One of the major engineering projects includes the new 7.2 km Leiderdorp-Hazerswoude tunnel under the Groene Hart (Green Heart) the agricultural area between the country's four largest cities, Amsterdam, Rotterdam, The Hague and Utrecht. North of this tunnel, a section of the line near the city of Rijpwetering, containing the sharpest curve on the entire route, experienced significant structural deformation during the construction stage due to ground instability, and 800 m of the line had to be rebuilt. The HSL has undergone two episodes of displacement. First one was just after the completion of the HSL construction. That falls into the period between 2nd null to 4th survey (Apr - Jun 2006). During this period some mitigation activities were carried out for slowing down and ceasing displacements; see Table 1. Following that period metal parts were repositioned on the top of concrete track. Soon, however, the second episode of displacement was emerged which corresponds to the period between 5th and 9th survey (Nov 2006 – Sep 2007). Local in-situ surveys show that up to 19 mm of horizontal deformation occurred after the construction stage in 2006.

In this respect, radar satellite interferometry is proved to be a valuable means for monitoring surface displacements due to subsidence, volcanic activities, earthquake and glacial motions (Massonnet and Feigl, 1998, Hanssen, 2001). But still, due to atmospheric disturbance, topography, temporal decorrelation, and unfavourable satellite orbital conditions, conventional interferometric methods are limited in their capability to estimate coherent surface deformation. In order to overcome these effects to a certain extent, Persistent Scatterer Interferometry techniques, see e.g., Ferretti et al. (2000, 2001) and Kampes (2006), were introduced. Persistent scatterers are radar reflections that behave coherently in time to provide reliable estimations of surface deformation that is up to mm level precision in the direction of the satellite line of sight (LOS). This technique has provided valuable information on the surface deformation pattern in varies test sites such as: subsidence due to gas extraction (Ketelaar et al, 2005), dike monitoring (Dentz et. al, 2006) and subsidence due to salt-mining (Humme, 2007).

With a similar approach, we investigate whether local deformation on the tracks of the HSL can be observed by satellite radar interferometry, using a fine-tuned processing technique dedicated for this application. In this study, we focus on the second episode of the displacement, i.e. Nov 2006 – Sep 2007, due to availability of coherent images.

Date	Survey	Activities
2006/04/04	1^{st} null	HSL construction phase is completed
2006/04/10	2^{nd} null	Extra (redundant) null measurement
2006/05/10	1^{st} repeat	Attachment of metal sheet piles
2006/06/16	2^{nd} repeat	1st phase pre-stress grout anchor
2006/08/02	3^{rd} repeat	2nd phase pre-stress grout anchor
2006/08/22	4^{th} repeat	rebuild top layer east side of the track
2006/10/25	5^{th} repeat	rebuild top layer west side of the track
2006/12/20	6^{th} repeat	
20070/2/16	7^{th} repeat	
2007/05/10	8^{th} repeat	
2007/09/07	9^{th} repeat	

Table 1 - Survey dates of HSL in relation to performed construction activities.

2. MODEL AND ANALYSIS

2.1. Forward Modelling of the radar line-of-sight deformation

In real life applications, unknown model parameters of an inverse problem usually exceed the number of observations. This causes a column rank defect in the system of equations, yielding them not uniquely solvable. More observations or simplified model equations with some assumptions may provide a solution. Here we use in-situ data in a forward model to obtain a first indication of the solvability of the inverse problem.

Using the three dimensional displacement vectors obtained from in-situ observations, the radar line-of-sight (LOS) displacement can be computed through a simple forward model. Let the surface displacement orthogonal components be $D = (d_x,d_y,d_z)$, in east, north, and vertical (up) directions, respectively, for a given point at the Earth's surface. Then, the projection of the surface displacement vector D to the line of sight can be formulated as:

$$d_{LOS} = \hat{s} \cdot D \tag{1}$$

$$\hat{s} = \left(-\cos\alpha_h \sin\theta \quad \sin\alpha_h \sin\theta \quad \cos\theta\right)^T \tag{2}$$

where d_{LOS}, $\hat{s}$, θ and α_h denote the line-of-sight displacement, the satellite unit vector, the radar incidence angle at the scattering point, and the azimuth heading of the satellite, respectively. It is worth noting in eq. (2) that surface uplift shows a positive LOS magnitude whereas subsidence shows negative values. The satellite LOS is roughly 9 and 4 times more sensitive to vertical displacements and the displacements in x (east) direction, respectively, compared to the component in the y (north) direction. This is due to the near-polar satellite orbits and the incidence angle of $\theta \cong 23$ degrees.

Displacements of the HSL (only in horizontal direction; it was assumed that no vertical deformation occurred) are estimated from repeated GPS and tachymetry measurements, see Table 1. Tachymetry measurements were crucial for reaching the required quality of measurement ordered by the Dutch Ministry of Transport and Public Works (Rijkswaterstaat). Survey contractor ARCADIS performed GPS and tachymetric surveys along a 1.4 km section of the HSL track for a period of two years, see Table 1. Some 220 measurement points were measured to detect displacements, of which 180 points were common throughout all survey epochs. Using those common points of measurements and, eqs. (1) and (2), we compute velocities in the radar LOS. Important parameters are the satellite heading α and incidence angle θ. We use nominal parameters for heading and incidence angle of an Envisat I2 descending pass. The simulation result of the forward model is illustrated in Figure 2. The simulation results indicate that the northern flank of the HSL track displaces toward East, whereas the southern flank displace towards West in the radar LOS. The bridge, which is located in the middle of the track, appears to be rather stable.

2.2. Persistent Scatterer Interferometry

Radar interferometry is based on computing phase differences, i.e. an interferogram, between repeated satellite acquisitions. An interferogram portrays not only phase differences due to displacements but also due to contributing factors such as atmospheric effects, temporal decorrelation, topography, and geometrical decorrelation. The degree of separability between these factors limits the feasibility of interferometric techniques to obtain coherent surface displacement.

PSI techniques use coherent and usually strong scatterers, known as Persistent Scatterers (PS), that provide coherent phase information over time for monitoring scatterer movement at millimetre level precision. Using PS points, atmospheric phase contributions can be estimated and filtered out through analysis of phase information in a stack of interferograms. This is due to the fact that atmospheric signal shows a specific spatial correlation, while it is uncorrelated in time (Hanssen, 1998). Conversely, displacements usually show a strong correlation in time, but may show lower correlation in space, dependent on the type of deformation. PSI techniques provide a relative measure of displacements in time, with respect to a reference (master) acquisition, and in space, with respect to a chosen reference point.

In our PSI processing, the area around the HSL's deforming rail track is analyzed using a series of 43 Envisat images covering the period August 2003 to October 2007. The master acquisition is chosen to be orbit 18012 (Aug 2005), providing maximum expected coherence for the whole series of interferograms. This is computed based on the perpendicular baselines, the temporal baselines and the mean Doppler centroid frequency differences. Additionally, it is selected among the master candidates closest in time to the date of the null survey.

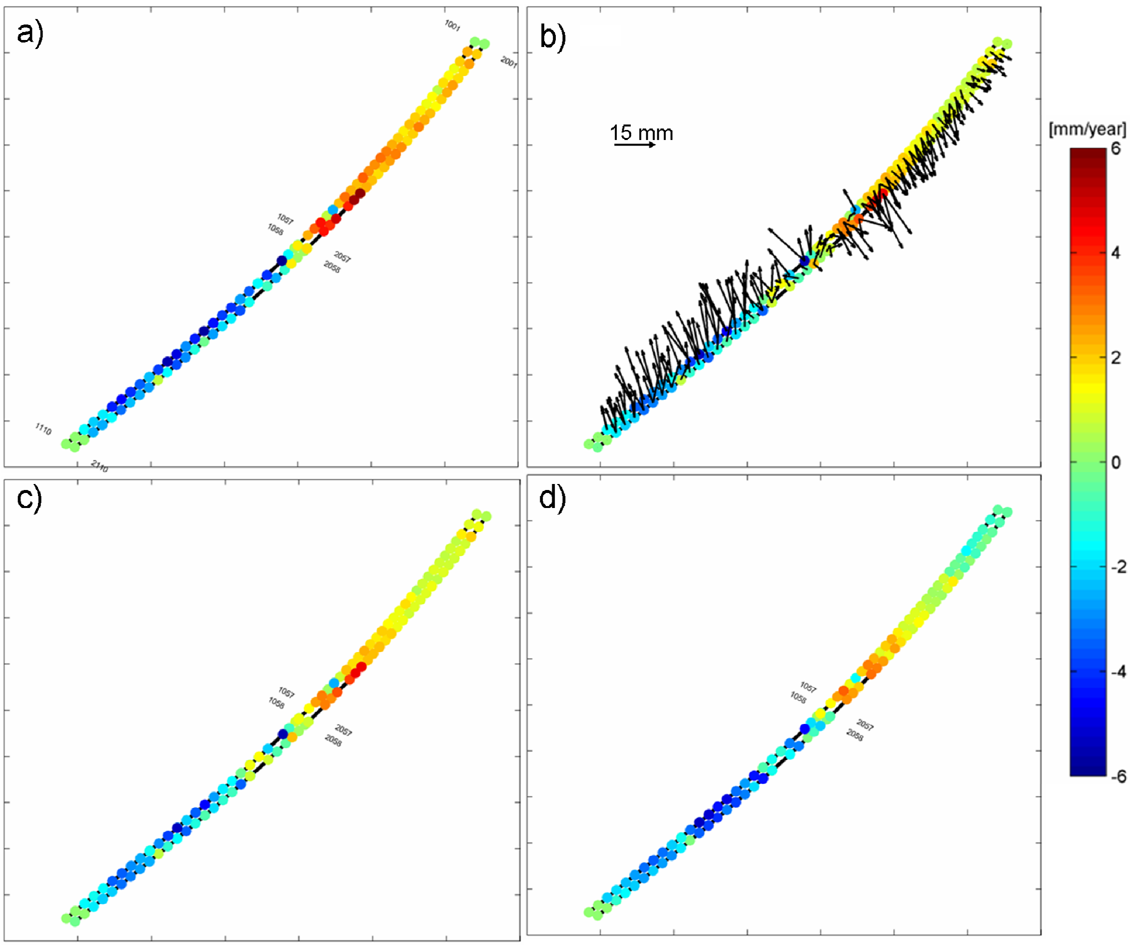

Figure 2 - The predicted satellite LOS displacements and velocities along the HSL track, based on the in-situ tachymetry observations. Numbers in the middle of the track indicate the location of the railway bridge. a) The LOS displacements at 9th repeat survey (Apr 2006 – Sep 2007) in mm. b) Predicted LOS velocities overlaid by horizontal displacement vectors between null and 9th repeat survey. c) Predicted LOS velocities between 2nd null survey and 9th repeat survey (Apr 2006 – Sep 2007). d) Predicted LOS velocities between the 5th and 9th repeat survey (Oct. 2006 – Sep. 2007).

First, using 42 computed interferograms, we select an initial set PS points based on a low amplitude dispersion (Ferretti et al., 2001) and a uniform spatial distribution (Kampes, 2006). These are strong scatterers that show consistent backscattering, and presumably coherent phase behaviour, over time. After first analysis and filtering, using those scatterers, we estimate the atmospheric phase screens (APS) of the consecutive acquisitions. Thus, the atmospheric phase contribution is removed for every pixel of every image in the time series. This approach ensures that we use the maximum amount of available acquisitions for APS estimation, which makes it most reliable. However, this series (Aug 2003 – Oct 2007) is too long for the deformation phenomenon, which took place between Apr 2006 and Sep 2007.

We focus our in-depth analysis on the time interval beginning just after re-construction of the west side of the rail track, in Oct 2006, see Table 1. In that period, we identify 8 acquisitions (Nov 2006 – Aug 2007) within the bounds of the survey activities, see Figure 3. Therefore, we expect to observe displacement along the HSL track via identical scatterers, which have not been disturbed over time by construction activities. Hence, no additive displacement is assumed to be introduced to the displacement of the HSL tracks.

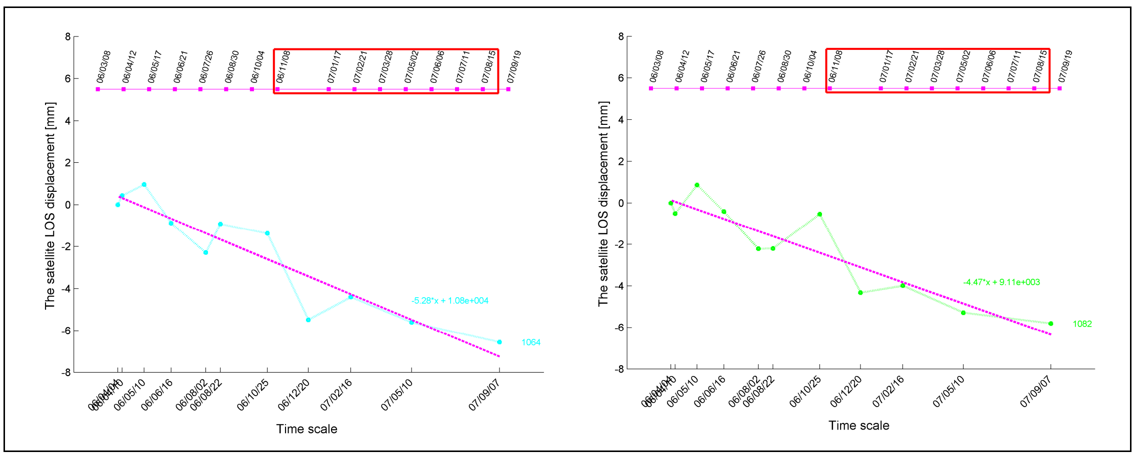

Figure 3 - The time series of the predicted LOS displacements computed using the in-situ tachymetry observations for the measurement points 1064 and 1082, respectively. The red box indicates that the dates of eight acquisitions used for estimation the displacement field in the PSI analysis.

In addition, we defined an area of interest mask in order to reveal the whole deformation pattern along the highly deforming part of the rail tracks. This mask is manually drawn using the multi-reflectivity radar map in a graphical environment. Within the mask, we process every pixel for displacements to increase the PS density on the rail track. This new set of PS points is instantly added to the existing set of PS points which were initially selected based on amplitude temporal variations. All PS were tested for their reliability by a misclosure test to three neighbouring points. Additionally, in our PS processing chain, we have limited our solution space by limiting topographical deviation and displacement deviation in the linear model in order to focus on the displacement along the HSL track. The displacement pattern has been illustrated in Figure 4.

In order to validate the displacement estimated by SAR observations, we use in-situ observations as a reference. First, we have linearly interpolated measurements, projected in the LOS for each acquisition date (Nov 2006 – Aug 2007) of the radar satellite. Then, using estimated displacements from PSI analysis and simulated LOS displacements, we sub-grouped each set of displacements into equal dimensional data blocks along the track, outlined in Fig 4b. For every epoch, we compute a spatial average displacement, see Figure

4b. Finally, we compute velocity and corresponding residuals between the displacement measurements and the linear velocity model, for statistical analysis, see Table 2.

3. RESULT AND DISCUSSIONS

Using a forward model simulation on the survey data, we translated horizontal motions to the satellite LOS assuming no elevation change, since in-situ data was lacking elevation measurements. It is clear that the southern part of the HSL bridge deforms faster than the northern part, and that the first and last surveyed points are relatively stable. The maximum satellite LOS displacement is observed, in the 9^{th} survey, with an amount of 6.6 mm at measurement point 1064, which is displaced horizontally 18 mm away from the satellite; see Figure 2b and Figure 2c. However, during the 9^{th} survey, the maximum horizontal displacement was measured with an amount of 19.2 mm which corresponds to -5.8 mm displacement in the radar LOS. This is due to the orientation of displacement vector with respect to the radar LOS for a descending orbit. The linear rates of displacement estimates for measurement points 1064 and 1082 are -5.3 and -4.5 mm/year, respectively, in the radar LOS. The displacement time series for these points are illustrated in Figure 3. These plots indicate that there has been some decrease in displacements after pre-stressing grout anchor phases and re-construction stages of top railway tracks; however, displacements continued, increasing in the following periods.

Polygon Block	Correlation of Average Displacement	Correlation of Displacement Residuals
1	0.92	0.25
2	-0.96	-0.33
3	0.87	-0.14
4	-0.97	-0.17
5	-0.98	-0.36
6	-0.96	-0.36
7	-0.28	-0.44
8	0.86	-0.49
9	0.91	-0.29
10	0.95	-0.24
11	0.93	-0.59

Table 2 - The time series correlation coefficients within each data block

In PS processing, we filtered out some noisy displacement estimates that may arise due to radar side lobes, which give erroneous information. Following that the correlation coefficient is computed between the displacement time series of simulated LOS measurements and PS estimates within each data block along the HSL track as a statistical measure, see Table 2. The coefficients are the indication of the magnitude and direction of a linear relation between two different sources of the displacement measurements. Negative values are an indication of decreasing linear relationship, which may be due to some noisy estimates left out in the PS results. The low correlation at the 7th data block corresponds to the part of the track where the magnitude and the direction of the displacement pattern change, see Figure 2 and Figure 4a. The northern part of the HSL shows negative correlation. That is, when the in-situ LOS measurements show an increasing trend, the PS estimates show a decreasing trend in the displacements. However, in the southern part of the HSL, both data sets show the same decreasing trend in the displacements. The mean of the velocities for the PS points in the northern part is -2.2 mm/year, whereas in the southern part it is -4.6 mm/year. The average displacement residuals show no significant relation, that is no linear dependencies between to two systems of measurments.

For the estimated linear LOS velocities, we computed variance-covariance matrix and presented in the following equation:

$$Q_{\hat{x}} = \begin{bmatrix} \sigma_t^2 & \sigma_{ts} \\ \sigma_{st} & \sigma_s^2 \end{bmatrix} = \begin{bmatrix} 0.70 & 5.33 \\ 5.33 & 40.56 \end{bmatrix} \tag{3}$$

where σ_t, σ_s, σ_{st} and σ_{ts} denote the variance of simulated LOS velocities, the variance of estimated PS velocities and their corresponding covariance values; *t* and *s* denote tachymetry and satellite data, respectively. Here, the estimated linear velocity from the PS points indicates a higher variance than the variance of the terrestrial-based LOS data. This can be explained by the noisy displacement estimates within PS velocities. The positive covariance value indicates that velocity rates are likely to change mutually in the same direction.

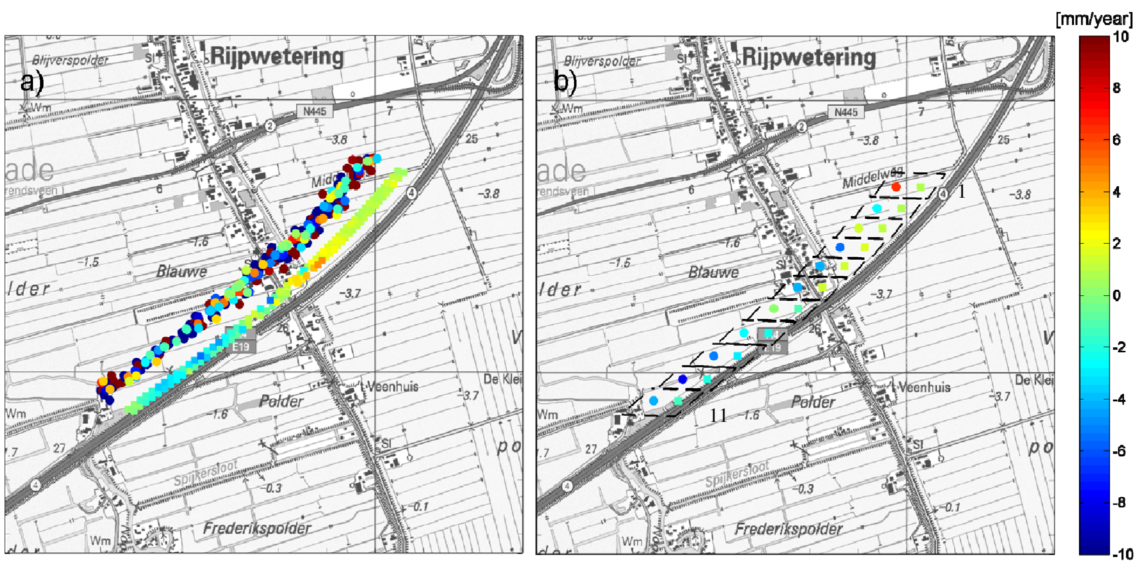

Figure 4 - The LOS velocities based on, the interpolated values of in-situ LOS displacements (in circles) between Nov 2006 and Aug 2007, and the estimated PS velocities (in squares), respectively. a) The predicted LOS velocities of all data points for each dataset. b) The average of LOS velocities within each polygon block for each dataset. Positional offset is introduced for visualizing purposes.

Several factors may affect the obtained results, such as, i) the selection of the master date, ii) the location of the reference point with in the master image, iii) model imperfections, iv) the selection of the time interval for analysis, and v) the availability of coherent data after the re-construction on the HSL track. Although the majority of the pixels appear to be noisy; there are points that show consistent behaviour similar to the simulated LOS displacements.

4. CONCLUSIONS

In this study we investigated the displacement pattern along the HSL construction using in-situ data and PSI techniques in the radar LOS. Using forward modelling and dedicated PS algorithms, we have evaluated every pixel along the relevant part of the HSL track for deformation. The main advantage of using PS technique is to benefit from pixels that are less like to suffer from temporal and geometrical decorrelation and in addition atmospheric phase delay can be estimated and subsequentially removed.

Time series LOS displacements are estimated between Nov 2006 and Aug 2007 using in-situ tachymetry data and InSAR images of a descending pass of Envisat. Although we obtained a comparable displacement pattern with in-situ data, the majority of pixels appear to be effected by the several factors from atmospheric disturbance, temporal decorrelation, topography, and geometrical decorrelation. Therefore, some valuable velocity estimations are diluted with noisy pixels, yielding biases in the estimations. Nevertheless, our results confirm the fact that the southern part of the track undergoes considerable deformation.

The deformation along the HSL underlines the importance of monitoring man made structures that are suspected to undergo deformation under ground instability. Without such in-situ information, SAR observations could be an important alternative to obtain reliable estimates of structural deformation. Further studies will be conducted to improve our analysis to detect such displacement in a more precise manner.

Acknowledgments

The authors would like to thank F. van Leijen and A. Amiri-Simkooei for valuable discussions during development and implementation of algorithms. We are grateful to The European Space Agency (ESA) for providing ENVISAT data and ARCADIS for providing tachymetry survey data. Interferometric data were processed using the public domain SAR processor DORIS, DORIS-PS, and satellite orbits from Delft University of Technology.

References

Dentz, F., van Halderen, L., Possel, B., Esfahany, S.S., Slobbe, C. and Wortel, T. (2006). *On the Potential of Satellite Radar Interferometry for Monitoring Dikes of the Netherlands.* Technical feasibility study. Delft University of Technology. Delft, the Netherlands.

Ferretti, A., Prati, C., and Rocca, F. (2000). Nonlinear subsidence rare estimation using permanent scatterers in differential SAR interferometry. *IEEE Transactions on Geoscience and Remote Sensing*, 38(5), p. 2202-2212.

Ferretti, A., Prati C., and Rocca, F. (2001). Permanent Scatterers in SAR Interferrometry, *IEEE Transactions on Geoscience and Remote Sensing*, 39(1), p. 8-20.

Hanssen, R.F. (2001). *Radar interferometry: Data interpretation and error analysis.* Dordrecht: Kluwer Academic Publishers

Hanssen, R.F. (1998). *Assessment of the role of atmospheric heterogeneities in ERS tandem SAR interferometry.* Technical report for the European Space Agency. Delft Institute for Earth-Oriented Space Research, Delft, the Netherlands.

Humme, A.J.M. (2007). *Point Density Optimization for SAR Interferrometry*, Msc. Thesis, Delft University of Technology. Delft, the Netherlands.

HSL-Zuid (no date). *Hoge Snelheids Lijn-Zuid.* at URL: http://www.hslzuid.nl (viewed 19/03/08).

Kampes, B.M. (2006). *Radar interferometry: Persistent Scatterer Technique.* Dordrecht: Kluwer Academic Publishers.

Ketelaar, V.B.H., van Leijen, F., Marinkovic, P., and Hanssen, R.F. (2005). On the use of point target characteristics in the estimation of low subsidence rates due to gas extraction in Groningen, the Netherlands. *In Fourth International Workshop on ERS/Envisat SAR Interferometry*, `FRINGE05', Frascati, Italy, 28 Nov-2 Dec 2005. ESA 2006, p. 6.

Massonnet D., and Feigl, K.L., 1998. *Radar interferometry and its application to changes in the earth's surface*. Reviews of Geophysics 36(4), p. 441-500.

Corresponding author contacts
Mahmut ARIKAN
M.Arikan@tudelft.nl
Delft Institute of Earth Observation and Space Systems
Delft, the Netherlands